

The Anglo-Australian Planet Search. XXIII. Two New Jupiter Analogs

Robert A. Wittenmyer^{1,2}, Jonathan Horner^{1,2}, C.G. Tinney^{1,2}, R.P. Butler³, H.R.A. Jones⁴, Mikko Tuomi^{4,5}, G.S. Salter^{1,2}, B.D. Carter⁶, F. Elliott Koch⁷, S.J. O’Toole⁸, J. Bailey^{1,2}, D. Wright^{1,2}

rob@phys.unsw.edu.au

ABSTRACT

We report the discovery of two long-period giant planets from the Anglo-Australian Planet Search. HD 154857c is in a multiple-planet system, while HD 114613b appears to be solitary. HD 114613b has an orbital period $P = 10.5$ years, and a minimum mass $m \sin i$ of $0.48M_{\text{Jup}}$; HD 154857c has $P = 9.5$ years and $m \sin i = 2.6M_{\text{Jup}}$. These new data confirm the planetary nature of the previously unconstrained long-period object in the HD 154857 system. We have performed detailed dynamical stability simulations which show that the HD 154857 two-planet system is stable on timescales of at least 10^8 yr. These results highlight the continued importance of “legacy” surveys with long observational baselines; these ongoing campaigns are critical for determining the population of Jupiter analogs, and hence of those planetary systems with architectures most like our own Solar system.

¹School of Physics, University of New South Wales, Sydney 2052, Australia

²Australian Centre for Astrobiology, University of New South Wales, Sydney 2052, Australia

³Department of Terrestrial Magnetism, Carnegie Institution of Washington, 5241 Broad Branch Road, NW, Washington, DC 20015-1305, USA

⁴University of Hertfordshire, Centre for Astrophysics Research, Science and Technology Research Institute, College Lane, AL10 9AB, Hatfield, UK

⁵University of Turku, Tuorla Observatory, Department of Physics and Astronomy, Väisäläntie 20, FI-21500, Piikkiö, Finland

⁶Computational Engineering and Science Research Centre, University of Southern Queensland, Toowoomba, Queensland 4350, Australia

⁷San Diego State University, Physics Department, 5500 Campanile Drive San Diego, CA 92182-1233, USA

⁸Australian Astronomical Observatory, PO Box 915, North Ryde, NSW 1670, Australia

Subject headings: planets and satellites: individual (HD 114613, HD 154857) – planets and satellites: detection – techniques: radial velocities – planets and satellites: dynamical evolution and stability

1. Introduction

A major theme that has unified exoplanet searches for more than 20 years is the question of how common (or rare) our own Solar system is. The *Kepler* spacecraft, which continuously monitored over 100,000 stars for tiny eclipses caused by orbiting planets (Borucki et al. 2010), has provided exquisite data which have revolutionised our understanding of the frequency of Earth-size planets in short-period orbits (Howard et al. 2012; Fressin et al. 2013). However, *Kepler* alone cannot give us a complete picture of the occurrence rate of planetary systems like our own, with rocky inner planets and one or more gas giant planets (“Jupiter analogs”) at orbital distances $a \gtrsim 3$ AU. There is more to a system being Solar System-like than having a single planet in a potentially habitable orbit. The detection of a Jupiter analog is a second key component in determining whether an exoplanetary system is Solar system-like. Over the years, many arguments have been put forth to suggest that such external giant planets might be a necessity for a potentially habitable exo-Earth to be a promising location for the development of life (Horner & Jones 2010a). Although the role of such planets acting as a shield from an otherwise damaging impact regime has come into question (e.g. Horner & Jones 2008; Horner et al. 2010; Lewis et al. 2013), a number of other potential benefits are thought to accrue from the presence of Jupiter-analogs. For example, Jupiter-like planets have been proposed as a solution to the question of the origin of Earth’s water. Current models of planetary formation suggest that the Earth formed in a region of the protoplanetary disk that was far too warm for water to condense from the gas phase. As such, it is challenging to explain the origin of our planet’s water without invoking an exogenic cause. The formation and evolution of the giant planets, beyond the snow line, offers a natural explanation for the delivery of volatiles from the cold depths of a planetary system to planets that move on potentially habitable orbits (e.g. Horner et al. 2009; Horner & Jones 2010b, and references therein). The detection of a Jupiter-analog is therefore both a second key component in determining whether an exoplanetary system is Solar system-like, and a potential marker that the planets in that system might be promising targets for the future search for life beyond the Solar system.

The Anglo-Australian Planet Search (AAPS) has been in operation for 15 years, and has achieved a long-term radial-velocity precision of 3 m s^{-1} or better since its inception, which is enabling the detection of long-period giant planets. To date, the AAPS has discovered

six Jupiter analogs: HD 70642b (Carter et al. 2003), HD 160691c (McCarthy et al. 2004), HD 30177b (Butler et al. 2006a), GJ 832b (Bailey et al. 2009), HD 134987c (Jones et al. 2010), HD 142c (Wittenmyer et al. 2012b). Here, we have defined a Jupiter analog as a giant planet which has ended up near its formation location, beyond the ice line, with $a > 3$ AU. Recently, the AAPS has shifted its priority to the detection of these Jupiter analogs. The observing strategy and target list have been modified, with the aim of producing an accurate and precise determination of the frequency of Jupiter-like planets in Jupiter-like orbits (Wittenmyer et al. 2011a, 2013b). The modified target list includes stars with long-term velocity stability such that Jupiter analogs can be robustly excluded (e.g. Wittenmyer et al. 2006, 2011b), as well as those stars with as-yet-incomplete orbits suggestive of long-period giant planets. In this paper, we report the discovery of two such Jupiter analogs with complete orbits. HD 154857 is already known to host a $1.8M_{\text{Jup}}$ planet with an orbital period of about 400 days (McCarthy et al. 2004); a residual velocity trend indicated a much longer-period object, as noted in the discovery work and in O’Toole et al. (2007).

This paper is organized as follows: Section 2 briefly describes the observational details and stellar parameters, and Section 3 details the orbit fitting process and gives the parameters of the two new planets. In Section 4, we present a dynamical stability analysis of the HD 154857 two-planet system, and we give our conclusions in Section 5.

2. Observations and Stellar Parameters

AAPS Doppler measurements are made with the UCLES echelle spectrograph (Diego et al. 1991). An iodine absorption cell provides wavelength calibration from 5000 to 6200 Å. The spectrograph point-spread function (PSF) and wavelength calibration are derived from the iodine absorption lines embedded on the spectrum by the cell (Valenti et al. 1995; Butler et al. 1996). The result is a precise Doppler velocity estimate for each epoch, along with an internal uncertainty estimate, which includes the effects of photon-counting uncertainties, residual errors in the spectrograph PSF model, and variation in the underlying spectrum between the iodine-free template and epoch spectra observed through the iodine cell. All velocities are measured relative to the zero-point defined by the template observation. For HD 114613, a total of 223 AAT observations have been obtained since 1998 Jan 16 (Table 1) and used in the following analysis, representing a data span of 5636 days (15.4 yr). The mean internal velocity uncertainty for these data is 0.94 m s^{-1} . HD 154857 has been observed 42 times since 2002 April (Table 2), for a total time span of 4109 days (11.3 yr) and a mean internal uncertainty of 1.71 m s^{-1} .

HD 114613 (HR 4979; HIP 64408) is an inactive G-type star, listed as a dwarf by Torres et al.

(2006), though its surface gravity is more indicative of a slightly evolved subgiant (Table 3). It is a nearby and bright star ($V = 4.85$) with a somewhat super-solar metallicity $[Fe/H] \sim 0.19$. HD 154857 has been classified as a G5 dwarf (Houk & Cowley 1975). However, all recent measurements of its surface gravity show that this star is a subgiant (Table 4). There is some confusion as to the mass: Valenti & Fischer (2005) give two disparate mass estimates, $2.10 \pm 0.31 M_{\odot}$ derived from spectroscopic analysis, and $1.27_{-0.29}^{+0.35} M_{\odot}$ from interpolation on a grid of Yonsei-Yale isochrones. For most stars in their sample, the two mass estimates agreed within $\sim 10\%$, but for HD 154857, they differ by almost a factor of 2. The more recent analysis by Takeda et al. (2007) yields an intermediate value of $1.718_{-0.022}^{+0.03} M_{\odot}$, which we adopt in this paper.

3. Orbit Fitting and Planetary Parameters

3.1. HD 114613

HD 114613 has been observed by the AAPS for the full 15 years of its operation. A long-period trend had been evident for several years, and in 2011, the trend resolved into a complete orbital cycle. We have since continued to observe HD 114613 to verify that the ~ 11 yr orbit was indeed turning around. Figure 2 shows the Generalized Lomb-Scargle periodogram (Zechmeister & Kürster 2009) of the 223 AAT observations. This type of periodogram weights the input data by their uncertainties, whereas the traditional Lomb-Scargle method (Lomb 1976; Scargle 1982) assumes uniform, Gaussian distributed uncertainties. To assess the significance of any signals appearing in these periodograms, we performed a bootstrap randomization process (Kürster et al. 1997). This randomly shuffles the velocity observations while keeping the times of observation fixed. The periodogram of this shuffled data set is then computed and its highest peak recorded. The longest-period peak near 4000 days is well-defined and highly significant, with a bootstrap false-alarm probability less than 10^{-5} . The next-highest peaks are at 122 and 1400 days, respectively. We fit these data with a single, long-period Keplerian using the *GaussFit* (Jefferys et al. 1988) nonlinear least-squares minimization routine. Jitter of 3.42 m s^{-1} (Wright 2005; O’Toole et al. 2009c) was added in quadrature to the uncertainties at each epoch prior to orbit fitting. A single-planet fit yields a period $P = 3825 \pm 106 \text{ d}$, $K = 5.4 \pm 0.4 \text{ m s}^{-1}$, and $e = 0.25 \pm 0.08$ (Table 5), making this planet a Jupiter analog (Wittenmyer et al. 2011a), with a minimum mass $m \sin i$ of $0.5 M_{\text{Jup}}$, and an orbital period of 10.7 years (Figure 1). The rms about the one-planet fit is 3.9 m s^{-1} , and the periodogram of the residuals to this fit is shown in the right panel of Figure 2, showing a number of peaks ranging from 28 to $\sim 1500 \text{ d}$.

There is structure evident in this residual periodogram (Figure 2, right panel), so we ex-

amined the residuals for additional Keplerian signals. One way of determining the veracity of such signals is to examine the data by seasons or subsets. This can disentangle true planetary signals (which would consistently appear in all subsets) from stochastic signals such as stellar rotational modulation (Dumusque et al. 2012; Hatzes 2013). We divided the residuals to the one-planet fit into two eight-season chunks. HD 114613 was observed intensely in 2007 and 2009 as part of the AAT “Rocky Planet Search” campaigns (O’Toole et al. 2009c,b), in which 24-30 bright stars were observed nightly for 48 continuous nights in search of short-period planets. It is possible that such a density of observational data may skew the false-alarm probabilities when evaluating potential additional signals. We thus removed the 66 epochs from the two “Rocky Planet Search” campaigns – this resulted in the 8-year halves containing 77 and 80 observations, respectively¹. Periodograms of the two halves are shown in Figure 3; visual inspection reveals that they are markedly different.

Table 6 shows the false-alarm probabilities obtained from 10,000 such realizations on each half of the 1-planet residuals. No periodicity is consistently significant in both subsets, with the possible exception of that near 27-29 days – however, this is worryingly close to both the 33-day rotation period of the star (Saar & Osten 1997) and the lunar month (at which the sampling of radial-velocity observations is well-known to impart spurious periodicities e.g. Dawson & Fabrycky 2010, Wittenmyer et al. 2013b). While it is tempting to consider a second planet near 1400 days, as found in the raw-data periodogram (Figure 2), we see that this signal is simply not evident in the first 8 years of observations. As suggested by (Hatzes 2013) for the proposed planet orbiting Alpha Centauri B, we rephrase his sentiments to express that any shorter period periodic signal which is evident in one subset of our data should also be evident in other subsets or seasons of the data. As both HD 114613 8-year subsets have ample time coverage and data quantity ($N = 77$) to sample the candidate periods listed in Table 6, we can use these results to conclude that there is not yet sufficient evidence for additional planetary signals in our data for HD 114613.

3.2. HD 154857

The presence of a planet orbiting HD 154857 was first reported by McCarthy et al. (2004), who noted that the AAPS data were best fit with the ~ 400 -day planet and a linear trend, indicating a more distant body. Additional data presented in O’Toole et al. (2007) refined the planet’s parameters and attempted to constrain the outer object’s orbit since the

¹Fitting a single planet with this shortened dataset gives parameters within 1σ of those given in Table 5, showing that the exclusion of those data do not affect our conclusions about the long-period planet.

residual velocity trend had begun to show curvature. They determined a minimum orbit with period 1900 days and $K \sim 23 \text{ m s}^{-1}$. Now, with a further 6 years of AAT data, the outer planet has completed an orbit and a double-Keplerian model converges easily. We used *GaussFit* as described above to fit the two planets, first adding jitter of 2.6 m s^{-1} in quadrature to the uncertainties (after O’Toole et al. 2007). The best-fit parameters are given in Table 5; the outer planet is a Jupiter analog moving on an essentially circular orbit with $P = 9.5 \text{ yr}$ ($a = 5.36 \text{ AU}$) and $m \sin i = 2.6 M_{\text{Jup}}$. The rms about the two-planet fit is 3.2 m s^{-1} , and there are no significant residual periodicities. The data and two-planet model are shown in Figure 4, and the orbital fits for the individual planets are shown in Figure 5.

4. Dynamical Stability Testing

Recent work has shown that any claim of multiple orbiting bodies must be checked by dynamical stability testing to ensure that the proposed planetary orbits are feasible on astronomically relevant timescales. Such testing can support the orbit fitting results (Robertson et al. 2012a; Wittenmyer et al. 2012b; Horner et al. 2012a), place further constraints on the planetary system configurations (Robertson et al. 2012b; Wittenmyer et al. 2012c; Tan et al. 2013), or show that the proposed planets cannot exist in or near the nominal best-fit orbits (Wittenmyer et al. 2012a; Goździewski et al. 2012; Horner et al. 2012b; Wittenmyer et al. 2013a; Horner et al. 2013). While HD 114613 appears to be a single-planet system, HD 154857 hosts two planets which are so widely separated (1.3 and 5.4 AU) that their dynamical interactions might be expected to be negligible. However, for completeness, we performed the dynamical analysis as in our previous work (Wittenmyer et al. 2012b).

We tested the dynamical stability of the HD 154857 system using the Hybrid integrator within the n-body dynamics package MERCURY (Chambers 1999). Holding the initial orbit of the innermost planet fixed, we tested $41 \times 41 \times 15 \times 5$ grid of “clones” spaced evenly across the 3σ range in the outer planet’s semi-major axis a , eccentricity e , periastron argument ω , and mean anomaly M , respectively.

In each integration, the orbital evolution of each planet was followed until it was either ejected from the planetary system (by reaching a barycentric distance of 10 AU), or collided with the central body or one of the other planets. The times at which such events occurred was recorded, which allowed us to construct a map of the stability of the HD 154857 planetary system as a function of the semi-major axis and eccentricity of the outer planet. As expected, the entire 3σ region exhibited stability for the full 10^8 yr . Indeed, not a single ejection or collision occurred in any of the 126,075 trial systems.

5. Discussion and Conclusions

We have described the detection of two Jupiter-analog planets from the 15-year Anglo-Australian Planet Search program. Our new data confirm the planetary nature of the previously unconstrained outer body in the HD 154857 system (McCarthy et al. 2004; O’Toole et al. 2007). These results highlight the importance of continuing “legacy” programs such as the AAPS, which is among the world’s longest-running radial-velocity planet searches. The planets detailed in this work bring the total number of AAPS-discovered Jupiter analogs to 8. With three Jupiter analogs confirmed in the past two years (HD 142c, Wittenmyer et al. 2012b; HD 114613b and HD 154857c, this work), the AAPS has nearly doubled its discoveries of these objects in years 14 and 15 of operation. We expect further discoveries of Jupiter analogs over the next few years as additional candidates complete orbits.

The AAPS has shifted its primary focus to the search for Jupiter analogs. Central to this strategy is the selection of a subset of ~ 120 targets (from the original 250-star AAPS sample) which satisfy two criteria: (1) sufficient observational baseline to detect a Jupiter analog, and (2) a sufficiently small velocity scatter to enable the robust detection of the $\sim 5\text{--}15\text{ m s}^{-1}$ signal produced by a Jupiter analog. Criterion (1) eliminates those stars added to the AAPS list well after its inception in 1998, and criterion (2) eliminates those stars which have high levels of intrinsic activity noise which would severely degrade the achievable detection limit. Using the detections and stringent limits from the *non-detections*, for every target we will be able to detect or exclude Jupiter analogs with high confidence. The result will be a direct measurement of the frequency of such objects, without suffering from significant incompleteness, which adds substantial uncertainty to this measurement (e.g. Cumming et al. 2008; Wittenmyer et al. 2011a).

There is an emerging correlation between debris disks and low-mass planets, first noted by Wyatt et al. (2012). They used *Herschel* to detect debris disks around 4 of 6 stars known to host only low-mass planets; no debris disks were found in the 5 systems hosting giant planets. One of the stars discussed here, HD 154857, has been observed for infrared excess (indicative of debris disks akin to the Solar system’s Edgeworth-Kuiper Belt). No excess was found from *Spitzer* and *Herschel* observations (Bryden et al. 2009; Dodson-Robinson et al. 2011). The HD 154857 system, hosting two giant planets and no detectable debris, is consistent with the pattern noted by Wyatt et al. (2012).

To obtain a complete picture of the nature of the planet candidates we have presented here, it would be ideal to determine true masses, rather than the minimum mass derived from radial-velocity measurements. Direct imaging offers a way forward: for stars known to host a long-period radial-velocity planet candidate, imaging can determine whether that object is stellar (i.e. detectable by imaging) or substellar. This type of characterization

has been done for some planet candidates, such as 14 Herculis c ($a > 7$ AU – Wittenmyer et al. 2007), for which AO imaging by Rodigas et al. (2011) established an upper limit of $42M_{\text{Jup}}$. The TRENDS survey (Crepp et al. 2012, 2013a,b) is currently using this strategy to target stars with known radial-velocity trends. The Gemini Planet Imager (GPI), now installed on the 8m Gemini South telescope (Hartung et al. 2013), has been specifically designed for the detection of these giant planets (McBride et al. 2011). It will provide not only the high contrasts needed to detect them, but also low-resolution spectra for each planet found, which can be used for their characterisation. We are now at a convergence of two developments in exoplanetary science: (1) radial-velocity data now extend comfortably into the range of Jupiter-analog orbital periods, and (2) direct imaging techniques have improved to the point where it is possible to detect Jupiter-like planets orbiting Sun-like stars at orbital distances approaching that of our own Jupiter (~ 5 AU). These complementary techniques can bridge the detectability gap, enabling direct measurements of the occurrence rate of Jupiter analogs orbiting Sun-like stars.

We thank the referee, William Cochran, for a timely report which improved this manuscript. This research is supported by Australian Research Council grants DP0774000 and DP130102695. This research has made use of NASA’s Astrophysics Data System (ADS), and the SIMBAD database, operated at CDS, Strasbourg, France. This research has also made use of the Exoplanet Orbit Database and the Exoplanet Data Explorer at exoplanets.org (Wright et al. 2011).

REFERENCES

- Bailey, J., Butler, R. P., Tinney, C. G., et al. 2009, *ApJ*, 690, 743
- Bond, J. C., Laretta, D. S., Tinney, C. G., et al. 2008, *ApJ*, 682, 1234
- Bond, J. C., Tinney, C. G., Butler, R. P., et al. 2006, *MNRAS*, 370, 163
- Borucki, W. J., Koch, D., Basri, G., et al. 2010, *Science*, 327, 977
- Bryden, G., Beichman, C. A., Carpenter, J. M., et al. 2009, *ApJ*, 705, 1226
- Butler, R. P., Marcy, G. W., Williams, E., McCarthy, C., Dosanjh, P., & Vogt, S. S. 1996, *PASP*, 108, 500
- Butler, R. P., Wright, J. T., Marcy, G. W., et al. 2006a, *ApJ*, 646, 505
- Butler, R. P., Wright, J. T., Marcy, G. W., et al. 2006b, *ApJ*, 646, 505

- Carter, B. D., Butler, R. P., Tinney, C. G., et al. 2003, *ApJ*, 593, L43
- Casagrande, L., Schönrich, R., Asplund, M., et al. 2011, *A&A*, 530, A138
- Chambers, J. E. 1999, *MNRAS*, 304, 793
- Crepp, J. R., Johnson, J. A., Howard, A. W., et al. 2012, *ApJ*, 761, 39
- Crepp, J. R., Johnson, J. A., Howard, A. W., et al. 2013a, *ApJ*, 771, 46
- Crepp, J. R., Johnson, J. A., Howard, A. W., et al. 2013b, *ApJ*, 774, 1
- Cumming, A., Butler, R. P., Marcy, G. W., Vogt, S. S., Wright, J. T., & Fischer, D. A. 2008, *PASP*, 120, 531
- Dawson, R. I., & Fabrycky, D. C. 2010, *ApJ*, 722, 937
- Diego, F., Charalambous, A., Fish, A. C., & Walker, D. D. 1990, *Proc. Soc. Photo-Opt. Instr. Eng.*, 1235, 562
- Dodson-Robinson, S. E., Beichman, C. A., Carpenter, J. M., & Bryden, G. 2011, *AJ*, 141, 11
- Dumusque, X., Pepe, F., Lovis, C., et al. 2012, *Nature*, 491, 207
- Fressin, F., Torres, G., Charbonneau, D., et al. 2013, *ApJ*, 766, 81
- Ghezzi, L., Cunha, K., Smith, V. V., et al. 2010, *ApJ*, 720, 1290
- Goździewski, K., Nasiroglu, I., Słowikowska, A., et al. 2012, *MNRAS*, 425, 930
- Gray, R. O., Corbally, C. J., Garrison, R. F., et al. 2006, *AJ*, 132, 161
- Hartung, M., Macintosh, B., Poyneer, L., et al. 2013, arXiv:1311.4423
- Hatzes, A. P. 2013, *ApJ*, 770, 133
- Henry, T. J., Soderblom, D. R., Donahue, R. A., & Baliunas, S. L. 1996, *AJ*, 111, 439
- Holmberg, J., Nordström, B., & Andersen, J. 2009, *A&A*, 501, 941
- Horne, J. H., & Baliunas, S. L. 1986, *ApJ*, 302, 757
- Horner, J., & Jones, B. W. 2008, *International Journal of Astrobiology*, 7, 251
- Horner, J., & Jones, B. W. 2009, *International Journal of Astrobiology*, 8, 75

- Horner, J., & Jones, B. W. 2010a, *International Journal of Astrobiology*, 9, 273
- Horner, J., & Jones, B. W. 2010b, *International Journal of Astrobiology*, 9, 273
- Horner, J., Jones, B. W., & Chambers, J. 2010, *International Journal of Astrobiology*, 9, 1
- Horner, J., Marshall, J. P., Wittenmyer, R. A., & Tinney, C. G. 2011, *MNRAS*, 416, L11
- Horner, J., Wittenmyer, R. A., Hinse, T. C., & Tinney, C. G. 2012a, *MNRAS*, 425, 749
- Horner, J., Hinse, T. C., Wittenmyer, R. A., Marshall, J. P., & Tinney, C. G. 2012b, *MNRAS*, 427, 2812
- Horner, J., Wittenmyer, R. A., Hinse, T. C., et al. 2013, arXiv:1307.7893
- Houk, N., & Cowley, A. P. 1975, *University of Michigan Catalogue of two-dimensional spectral types for the HD stars. Volume I. Declinations -90° to -53°, by Houk, N.; Cowley, A. P.*. Ann Arbor, MI (USA): Department of Astronomy, University of Michigan, 19 + 452 p.,
- Houk, N. 1982, *Michigan Catalogue of Two-dimensional Spectral Types for the HD stars. Volume_3. Declinations -40° to -26°, by Houk, N.*. Ann Arbor, MI(USA): Department of Astronomy, University of Michigan, 12 + 390 p.,
- Howard, A. W., Johnson, J. A., Marcy, G. W., et al. 2011, *ApJ*, 730, 10
- Howard, A. W., Marcy, G. W., Bryson, S. T., et al. 2012, *ApJS*, 201, 15
- Jefferys, W. H., Fitzpatrick, M. J., & McArthur, B. E. 1988, *Celestial Mechanics*, 41, 39
- Jenkins, J. S., Jones, H. R. A., Tinney, C. G., et al. 2006, *MNRAS*, 372, 163
- Jones, H. R. A., et al. 2010, *MNRAS*, 403, 1703
- Kürster, M., Schmitt, J. H. M. M., Cutispoto, G., & Dennerl, K. 1997, *A&A*, 320, 831
- Lawler, S. M., Beichman, C. A., Bryden, G., et al. 2009, *ApJ*, 705, 89
- Lewis, A. R., Quinn, T., & Kaib, N. A. 2013, *AJ*, 146, 16
- Lomb, N. R. 1976, *Ap&SS*, 39, 447
- Lykawka, P. S., & Mukai, T. 2007, *Icarus*, 192, 238
- Lykawka, P. S. 2012, *Monographs on Environment, Earth and Planets*, 1, 121

- Maldonado, J., Eiroa, C., Villaver, E., Montesinos, B., & Mora, A. 2012, *A&A*, 541, A40
- Marshall, J., Horner, J., & Carter, A. 2010, *International Journal of Astrobiology*, 9, 259
- McBride, J., Graham, J. R., Macintosh, B., et al. 2011, *PASP*, 123, 692
- McCarthy, C., Butler, R. P., Tinney, C. G., et al. 2004, *ApJ*, 617, 575
- O’Toole, S. J., Butler, R. P., Tinney, C. G., et al. 2007, *ApJ*, 660, 1636
- O’Toole, S. J., Tinney, C. G., Jones, H. R. A., et al. 2009a, *MNRAS*, 392, 641
- O’Toole, S., et al. 2009b, *ApJ*, 697, 1263
- O’Toole, S., et al. 2009, *ApJ*, 701, 1732
- Pepe, F., Lovis, C., Ségransan, D., et al. 2011, *A&A*, 534, A58
- Robertson, P., Endl, M., Cochran, W. D., et al. 2012a, *ApJ*, 749, 39
- Robertson, P., Horner, J., Wittenmyer, R. A., et al. 2012b, *ApJ*, 754, 50
- Rodigas, T. J., Males, J. R., Hinz, P. M., Mamajek, E. E., & Knox, R. P. 2011, *ApJ*, 732, 10
- Saar, S. H., & Osten, R. A. 1997, *MNRAS*, 284, 803
- Scargle, J. D. 1982, *ApJ*, 263, 835
- Sousa, S. G., Santos, N. C., Mayor, M., et al. 2008, *A&A*, 487, 373
- Takeda, G., Ford, E. B., Sills, A., et al. 2007, *ApJS*, 168, 297
- Tan, X., Payne, M. J., Hoi Lee, M., et al. 2013, arXiv:1306.0687
- Torres, C. A. O., Quast, G. R., da Silva, L., et al. 2006, *A&A*, 460, 695
- Torres, G., Andersen, J., & Giménez, A. 2010, *A&A Rev.*, 18, 67
- Valenti, J. A., Butler, R. P. & Marcy, G. W. 1995, *PASP*, 107, 966.
- Valenti, J. A., & Fischer, D. A. 2005, *ApJS*, 159, 141
- van Leeuwen, F. 2007, *A&A*, 474, 653
- Wittenmyer, R. A., Endl, M., Cochran, W. D., Hatzes, A. P., Walker, G. A. H., Yang, S. L. S., & Paulson, D. B. 2006, *AJ*, 132, 177

- Wittenmyer, R. A., Endl, M., & Cochran, W. D. 2007, *ApJ*, 654, 625
- Wittenmyer, R. A., Tinney, C. G., O’Toole, S. J., Jones, H. R. A., Butler, R. P., Carter, B. D., & Bailey, J. 2011, *ApJ*, 727, 102
- Wittenmyer, R. A., Tinney, C. G., Butler, R. P., et al. 2011b, *ApJ*, 738, 81
- Wittenmyer, R. A., Horner, J., Marshall, J. P., Butters, O. W., & Tinney, C. G. 2012, *MNRAS*, 419, 3258
- Wittenmyer, R. A., Horner, J., Tuomi, M., et al. 2012b, *ApJ*, 753, 169
- Wittenmyer, R. A., Horner, J., & Tinney, C. G. 2012c, *ApJ*, 761, 165
- Wittenmyer, R. A., Horner, J., & Marshall, J. P. 2013a, *MNRAS*, 1006
- Wittenmyer, R. A., Tinney, C. G., Horner, J., et al. 2013b, *PASP*, 125, 351
- Wright, J. T. 2005, *PASP*, 117, 657
- Wright, J. T., et al. 2011, *PASP*, 123, 412
- Wyatt, M. C., Kennedy, G., Sibthorpe, B., et al. 2012, *MNRAS*, 424, 1206
- Zechmeister, M., Kürster, M. 2009, *A&A*, 496, 577

Table 1. AAT/UCLES Radial Velocities for HD 114613

JD-2400000	Velocity (m s^{-1})	Uncertainty (m s^{-1})
50830.25655	4.0	1.2
50833.22381	1.9	0.8
50915.08074	0.6	1.4
50917.08662	-7.5	1.6
50970.91681	-11.8	1.1
51002.86733	-5.6	1.8
51212.26513	5.6	1.4
51236.21281	-5.5	1.4
51237.18130	-7.5	1.8
51274.21875	-1.8	2.0
51276.08909	-0.2	1.3
51382.92476	-3.9	1.2
51386.85182	1.8	1.2
51631.24051	-1.9	1.3
51682.84034	1.3	1.4
51684.05975	-2.8	1.4
51717.83623	-0.1	1.3
51919.25519	-0.8	1.8
51920.26898	-1.7	1.5
51984.11127	0.3	1.7
52061.03012	5.0	1.4
52062.09081	3.8	1.5
52092.95741	3.6	1.1
52127.88681	0.4	1.7
52359.20083	2.3	1.0
52387.02810	4.4	1.4
52388.06604	3.4	1.5
52509.86723	13.4	1.3
52510.86704	11.2	1.5
52654.26882	4.6	1.4
52710.14699	8.8	1.0
52710.95867	6.4	2.0
52745.09064	16.9	1.3
52751.11506	9.0	1.4
52752.07289	11.6	1.1
52783.95975	11.8	1.2
52785.05762	9.3	1.7
52785.97105	15.2	1.4
52857.87314	0.6	1.3
53008.22116	11.7	1.3
53041.22754	8.0	1.3
53042.22343	4.2	1.2
53046.15053	5.2	1.5
53051.15875	-0.3	1.0
53214.87828	10.8	1.0
53215.88215	9.6	1.2

Table 1—Continued

JD-2400000	Velocity (m s^{-1})	Uncertainty (m s^{-1})
53242.89915	4.5	0.8
53245.84896	14.4	1.5
53399.27632	5.5	0.6
53405.20308	2.0	0.7
53482.95081	-1.3	0.8
53484.04090	-4.9	0.7
53485.02218	-0.9	0.7
53485.94007	0.0	0.7
53486.06578	-0.8	0.7
53488.12718	1.2	0.7
53489.07405	-0.4	0.7
53506.95930	1.5	0.7
53507.88240	0.4	0.7
53509.07069	-4.2	0.7
53516.02470	2.0	1.0
53517.00282	6.4	0.8
53518.95553	6.2	0.7
53520.02670	6.0	0.8
53521.01119	7.7	0.8
53521.93055	4.4	0.9
53522.97922	4.0	0.8
53568.93024	1.4	0.7
53569.89040	-2.5	0.8
53570.93229	-0.1	0.7
53571.92818	4.4	0.7
53572.93960	3.5	0.6
53573.86024	2.8	0.7
53575.86501	4.8	0.6
53576.83855	1.5	0.6
53577.85712	0.4	0.9
53578.87161	1.6	0.6
53840.18077	-2.4	0.9
53841.14463	2.1	0.8
53843.11871	0.4	0.8
53844.06189	1.7	0.7
53937.92281	-1.6	0.7
53938.90015	1.4	0.6
53943.85615	-4.9	0.6
53944.87540	-7.3	0.6
53945.86861	-4.3	0.8
53946.86415	-7.3	0.6
54111.19771	3.5	0.6
54112.20754	4.7	0.8
54113.22282	3.5	0.8
54114.24651	2.6	0.9
54115.25260	3.5	1.2

Table 1—Continued

JD-2400000	Velocity (m s^{-1})	Uncertainty (m s^{-1})
54120.20490	7.7	0.7
54121.19705	3.8	0.6
54123.22186	9.1	0.6
54126.18385	2.7	0.7
54127.18893	5.0	0.5
54128.18767	4.0	0.8
54129.18497	-0.7	0.5
54130.17738	0.9	0.7
54131.18561	2.0	0.6
54132.19227	2.1	0.8
54133.25166	1.4	1.1
54134.21614	4.1	0.6
54135.18151	-1.1	0.7
54136.20085	0.8	0.6
54137.19842	1.3	0.6
54138.17883	0.1	0.9
54139.17104	3.0	0.8
54140.17481	-0.1	0.8
54141.20213	-1.6	0.8
54142.19235	0.6	0.5
54144.12894	-3.4	0.6
54145.15798	-2.9	0.6
54146.17863	-0.3	0.6
54147.19558	-3.5	0.6
54148.22623	-2.7	0.6
54149.16439	-2.0	0.6
54150.19348	-1.7	0.6
54151.20779	-3.0	0.6
54152.22033	-2.7	0.7
54154.19334	-5.2	0.6
54155.19519	-3.2	0.7
54156.16473	-1.3	0.6
54223.10365	1.9	0.9
54224.14365	1.1	0.8
54225.07630	1.8	0.7
54226.00805	1.9	1.0
54227.04258	5.5	0.8
54252.96645	9.5	0.9
54254.00991	9.0	0.8
54254.91285	5.6	0.9
54255.97533	3.7	0.9
54257.06303	5.6	0.9
54333.85357	3.5	0.9
54334.87415	2.6	0.9
54335.86542	2.5	0.7
54336.85846	6.7	0.8

Table 1—Continued

JD-2400000	Velocity (m s^{-1})	Uncertainty (m s^{-1})
54543.05240	0.0	0.8
54544.14396	-0.8	0.8
54550.09556	-1.0	1.4
54551.09203	-1.9	0.9
54552.13245	3.0	1.1
54553.10244	-3.6	1.1
54841.25120	-0.4	1.0
54897.20442	-8.4	1.0
54900.18137	-12.3	1.2
54901.15823	-6.8	0.9
54902.20552	-10.1	1.0
54904.19780	-6.0	1.0
54905.26523	-1.6	0.8
54906.21006	-5.8	1.0
54907.19989	-6.8	0.9
54908.20498	-6.8	0.8
55014.94187	-6.2	1.0
55015.86595	-4.9	0.8
55018.84451	1.4	1.9
55019.87410	-5.8	0.7
55020.84762	-6.3	0.7
55021.87399	-7.7	0.8
55022.88779	-10.4	0.8
55023.86739	-11.0	0.9
55029.84869	-6.6	0.6
55030.83778	-4.0	0.7
55031.90051	-3.4	0.7
55032.91264	-3.6	0.6
55036.84785	-6.2	0.7
55037.83638	-2.9	0.7
55040.84113	-6.1	0.8
55041.85626	-6.0	0.9
55043.88548	-3.7	0.6
55044.85993	-4.9	0.6
55045.85496	-5.0	0.5
55046.90149	-6.5	0.7
55047.88023	-4.0	0.5
55048.86964	-5.4	0.5
55049.85230	-4.1	1.0
55050.85220	-7.8	0.8
55051.84966	-5.0	0.5
55053.85289	-8.7	0.6
55054.84736	-8.0	0.6
55055.88706	-6.2	0.5
55058.87417	-4.9	0.6
55206.19055	-2.4	0.8

Table 1—Continued

JD-2400000	Velocity (m s^{-1})	Uncertainty (m s^{-1})
55209.20056	-1.9	0.8
55253.19939	-6.9	0.9
55254.28349	-9.6	1.0
55310.06142	2.1	0.8
55312.07035	-2.4	0.8
55317.03644	-5.0	0.9
55370.94153	3.1	1.0
55374.90773	0.7	1.0
55397.89284	-6.3	1.0
55402.84315	-5.0	0.7
55586.21266	0.8	0.9
55603.27577	3.8	1.1
55604.27940	-0.2	1.1
55663.95088	0.5	1.1
55666.06790	2.5	0.9
55692.08906	0.5	1.1
55692.97915	5.8	0.9
55750.89289	-3.6	0.8
55751.87344	-2.2	1.3
55753.84964	-3.0	1.0
55756.87098	-1.2	1.1
55785.90110	2.3	1.0
55786.86812	4.9	1.5
55787.92128	5.1	1.1
55961.17818	-0.1	0.8
55964.22153	6.2	0.8
55996.09776	-3.3	0.9
56049.03768	2.1	1.1
56051.03503	-0.1	1.1
56084.99567	9.3	1.3
56085.98717	3.6	1.1
56134.98050	6.9	1.2
56138.89373	3.4	1.1
56379.13086	2.6	1.3
56382.21632	10.6	1.9
56383.07275	1.5	0.8
56464.91329	10.2	1.1
56465.92701	9.3	0.9
56466.91347	8.0	0.9

Table 2. AAT/UCLES Radial Velocities for HD 154857

JD-2400000	Velocity (m s^{-1})	Uncertainty (m s^{-1})
52389.23580	-3.3	1.7
52390.21223	-4.9	1.5
52422.13713	-17.3	1.5
52453.01957	-14.2	1.4
52455.02535	-13.7	1.9
52455.97664	-12.2	1.9
52509.94853	-16.3	2.1
52510.91619	-6.6	1.8
52711.24602	63.7	2.8
52745.24271	66.4	1.9
52747.21175	58.7	1.8
52750.17761	52.7	1.5
52751.22944	47.2	1.4
52784.12626	-11.5	1.3
52857.02974	-28.4	2.7
52857.98599	-31.9	1.4
52942.91225	-18.1	1.7
53217.01252	-41.2	1.5
53246.03809	-53.3	1.9
53485.15229	21.5	1.5
53510.15968	25.9	1.4
53523.10133	33.2	1.5
53570.02945	32.9	2.3
53843.23961	-7.0	1.6
53945.03237	49.6	1.0
54008.89626	-21.4	0.9
54037.88134	-39.5	1.4
54156.28808	-17.5	1.9
54226.21678	-2.3	1.2
54254.99229	5.5	1.6
54372.93185	61.1	1.3
54552.23398	-9.0	2.2
54901.28209	-7.9	2.1
55101.89348	54.8	1.7
55313.23386	2.5	1.4
55317.13834	1.1	1.7
55399.04324	17.8	1.4
55429.91942	23.9	1.3
56049.24780	1.1	2.1
56465.07924	-22.4	1.9
56467.06137	-20.2	1.7
56498.02816	-40.6	3.0

Table 3. Stellar Parameters for HD 114613

Parameter	Value	Reference
Spec. Type	G4IV	Gray et al. (2006)
	G3V	Torres et al. (2006)
Mass (M_{\odot})	1.364	Sousa et al. (2008)
Distance (pc)	20.67 ± 0.13	van Leeuwen (2007)
$V \sin i$ (km s^{-1})	2.7 ± 0.9	Saar & Osten (1997)
$\log R'_{HK}$	-5.118	Gray et al. (2006)
$[Fe/H]$	0.19 ± 0.01	Sousa et al. (2008)
	0.18	Maldonado et al. (2012)
$[O/H]$	0.03 ± 0.01	Bond et al. (2008)
$[Cr/H]$	0.09 ± 0.04	Bond et al. (2008)
$[Mg/H]$	-0.04 ± 0.06	Bond et al. (2008)
$[Zr/H]$	0.17 ± 0.04	Bond et al. (2008)
$[Eu/H]$	-0.17 ± 0.04	Bond et al. (2008)
$[Nd/H]$	0.05 ± 0.01	Bond et al. (2008)
$[Si/H]$	0.19 ± 0.06	Bond et al. (2006)
T_{eff} (K)	5729 ± 17	Sousa et al. (2008)
	5574	Gray et al. (2006)
	5550	Saar & Osten (1997)
$\log g$	3.97 ± 0.02	Sousa et al. (2008)
	3.90	Gray et al. (2006)

Table 4. Stellar Parameters for HD 154857

Parameter	Value	Reference
Spec. Type	G5V	Houk & Cowley (1975)
Mass (M_{\odot})	$1.718^{+0.03}_{-0.022}$	Takeda et al. (2007)
Distance (pc)	64.2 ± 3.1	van Leeuwen (2007)
$V \sin i$ (km s^{-1})	1.4 ± 0.5	Butler et al. (2006b)
$\log R'_{HK}$	-5.00	Jenkins et al. (2006)
	-5.14	Henry et al. (1996)
[Fe/H]	-0.31	Holmberg et al. (2009)
	-0.30	Ghezzi et al. (2010)
	-0.22	Valenti & Fischer (2005)
	-0.20	Casagrande et al. (2011)
[O/H]	-0.15 ± 0.03	Bond et al. (2008)
[Cr/H]	-0.20 ± 0.04	Bond et al. (2008)
[Mg/H]	-0.20 ± 0.03	Bond et al. (2008)
[Zr/H]	-0.08 ± 0.04	Bond et al. (2008)
[Eu/H]	-0.27 ± 0.07	Bond et al. (2008)
[Nd/H]	-0.01 ± 0.02	Bond et al. (2008)
[C/H]	-0.28 ± 0.07	Bond et al. (2006)
[Si/H]	-0.28 ± 0.11	Bond et al. (2006)
T_{eff} (K)	5605	Dodson-Robinson et al. (2011)
	5508	Holmberg et al. (2009)
	5548	Ghezzi et al. (2010)
$\log g$	$3.95^{+0.05}_{-0.03}$	Takeda et al. (2007)
	3.82	Ghezzi et al. (2010)
	3.99 ± 0.06	Valenti & Fischer (2005)
Radius (R_{\odot})	$2.31^{+0.17}_{-0.10}$	Takeda et al. (2007)
	1.760 ± 0.057	Torres et al. (2010)

Table 5. Keplerian Orbital Solutions

Planet	Period (days)	T_0 (JD-2400000)	e	ω (degrees)	K (m s^{-1})	$m \sin i$ (M_{Jup})	a (AU)	χ^2_{ν}
HD 114613 b	3827 ± 105	$55550.3 \pm (\text{fixed})$	0.25 ± 0.08	244 ± 5	5.52 ± 0.40	0.48 ± 0.04	5.16 ± 0.13	1.23
HD 154857 b	408.6 ± 0.5	53572.5 ± 2.4	0.46 ± 0.02	57 ± 4	48.3 ± 1.0	2.24 ± 0.05	1.291 ± 0.008	1.35
HD 154857 c	3452 ± 105	55219 ± 375	0.06 ± 0.05	352 ± 37	24.2 ± 1.1	2.58 ± 0.16	5.36 ± 0.09	

Table 6. Candidate Secondary Signals for HD 114613

First Half		Second Half	
Period (days)	FAP	Period (days)	FAP
28.9	0.015	26.6	0.0001
72.5	0.952	73.3	0.1836
122	1.000	121.4	0.0246
490.2	0.138	480.8	0.9755
1562.5	0.910	1111.1	0.0003

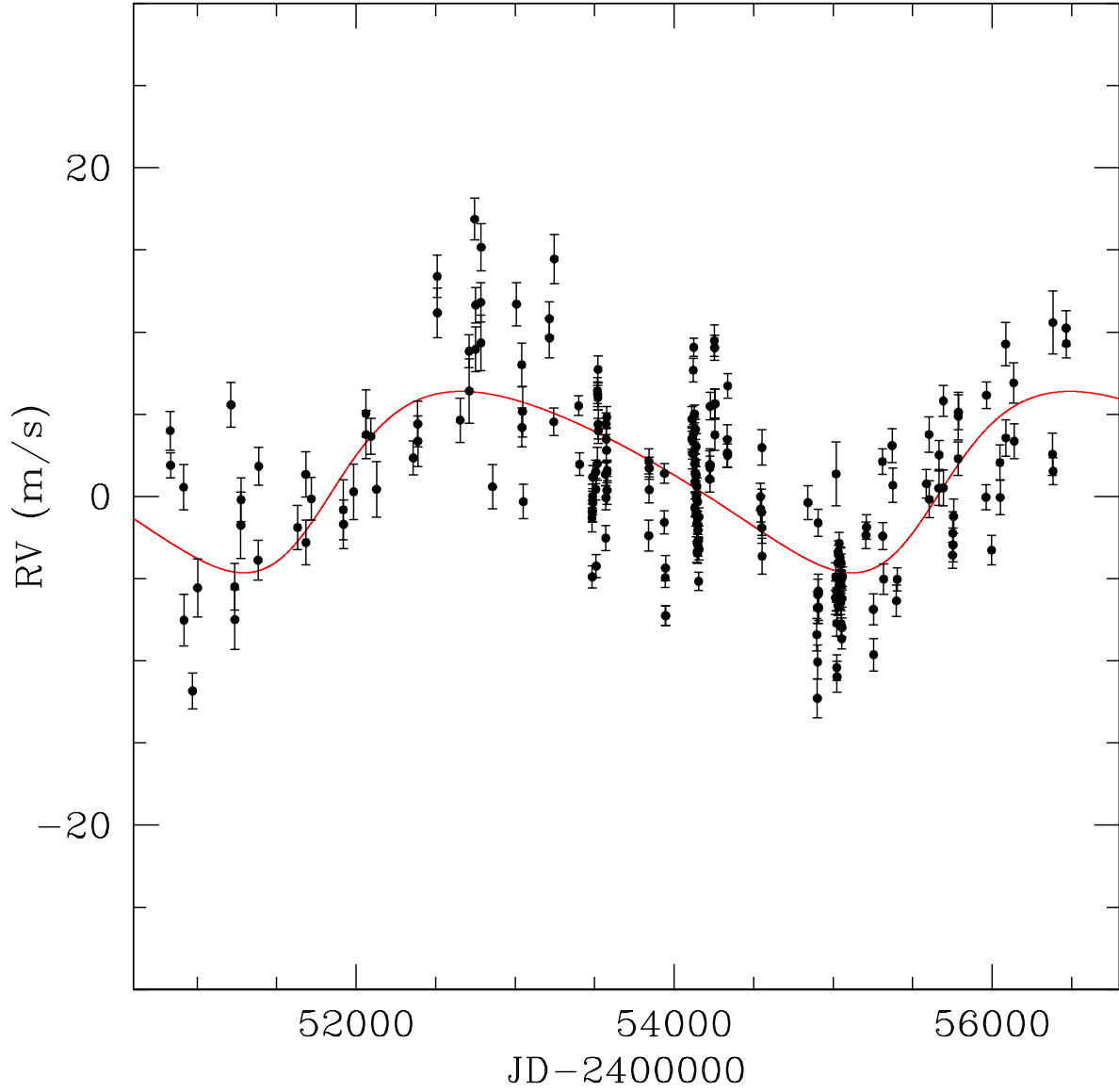


Fig. 1.— Keplerian orbit fit for HD 114613b. The planet has completed about 1.5 cycles, and the AAT data show a residual rms scatter of 3.9 m s^{-1} .

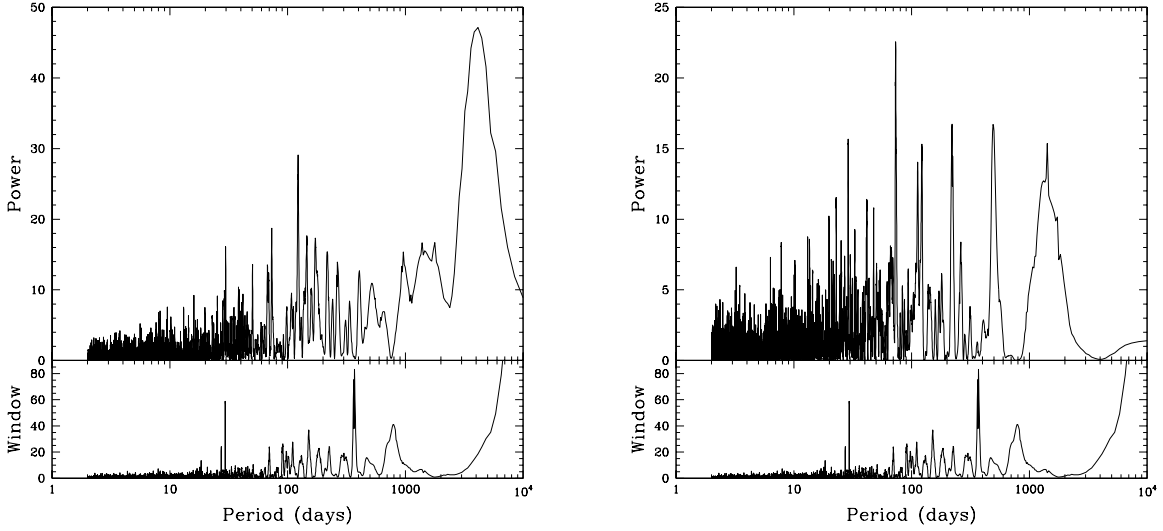


Fig. 2.— Left: Generalized Lomb-Scargle periodogram of 223 AAT observations of HD 114613. A highly significant peak is present near 4000 days. Right: Periodogram of the residuals after fitting and removing the long-period planet with the parameters given in Table 5; several peaks remain which may indicate further planets.

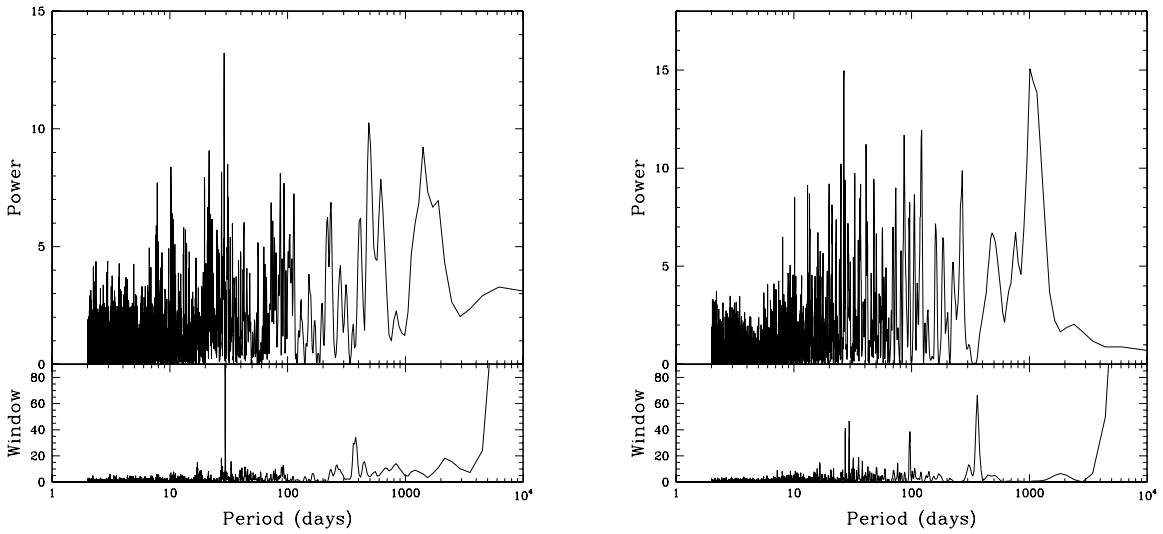


Fig. 3.— Periodograms of the residuals to a single-planet fit for HD 114613. Left: First eight years ($N = 77$). Right: Second eight years ($N = 80$), excluding the high-cadence observing runs in 2007 and 2009.

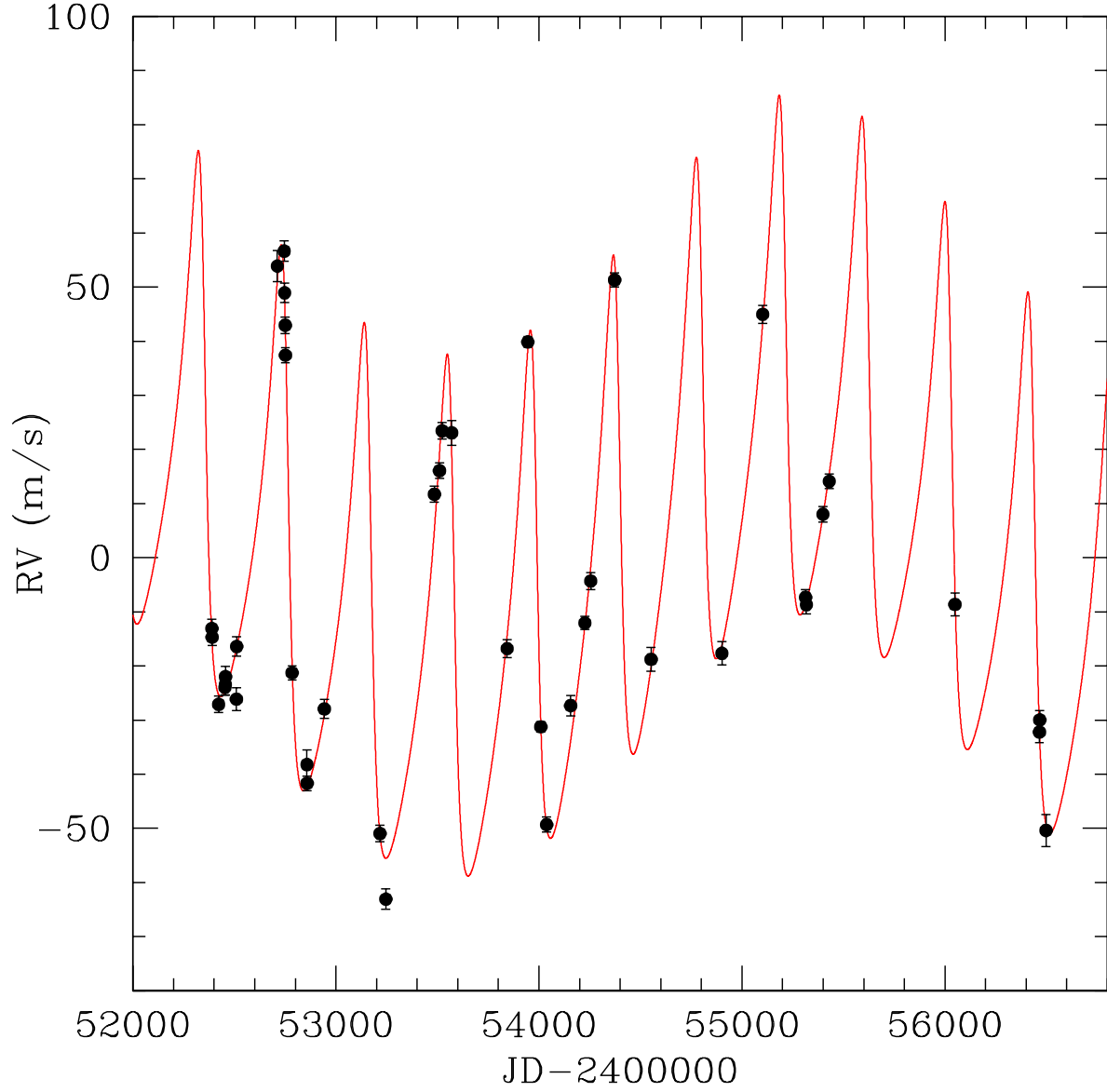


Fig. 4.— Two-planet Keplerian model and AAT data for the HD 154857 system. The rms about this fit is 3.2m s^{-1} .

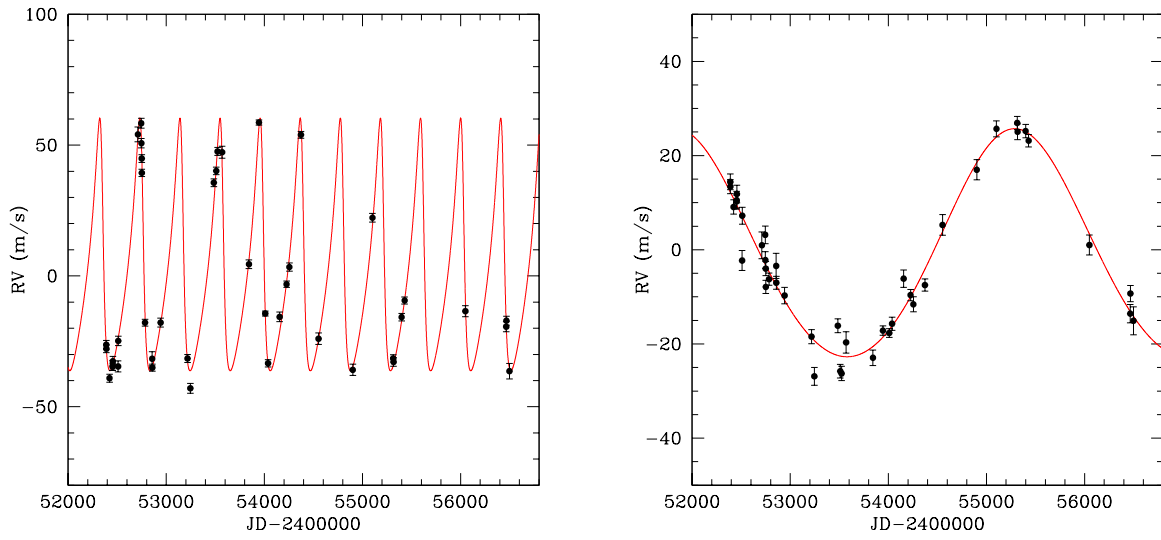


Fig. 5.— Left: Data and model fit for HD 154857b; the signal of the outer planet has been removed. Right: Same, but for HD 154857c after removing the inner planet.